International Journal of Environmental Science and Technology (2024) 21:3943–3956
https://doi.org/10.1007/s13762-023-05256-2

ORIGINAL PAPER

A comparative study of drinking straws made from natural resources: structural and morphological characterization

E. Tarani[1] · **K. Chrissafis**[1]

Received: 11 October 2022 / Revised: 9 June 2023 / Accepted: 4 October 2023 / Published online: 27 October 2023

Abstract

This study focuses on identifying a high-value material using low-cost raw resources by comparing wheat straw varieties collected in Greece with other commercial straws made of reed, bamboo, paper, and bioplastic. The structural characteristics, water absorption behavior, and morphological properties of the straws were analyzed using X-ray diffraction, water immersion tests, and scanning electron microscopy. The thermal degradation was investigated using thermogravimetric analysis. The results suggest that the wheat straws exhibit a significant degree of crystallinity, with the Staramaki K1 straw exhibiting the highest crystallinity of all the straws analyzed. The mass of wheat straws increased after immersion in water, coca-cola, and fresh orange juice in contrast to the mass of bioplastic and bamboo straws, which remained constant. The surface examination revealed modifications to the straws' outer and inner surfaces after immersion in the various solutions. To variable degrees, pores, cracks, peeling material, lighter patches, and anomalies were seen. The presence of a highly crystalline structure can increase the straw's hardness and reduce its water absorption, making it more resistant to changes brought about by the solutions. So, the Staramaki K1 wheat straw exhibits favorable properties, including high crystallinity, lower water absorption, and thermal stability, making it a promising candidate for replacing conventional plastic drinking straws.

Keywords Absorption · Crystallinity · Stability · Staramaki · Surface · Sustainability · Wheat straw

Introduction

Plastic pollution is a major environmental hazard that is responsible for a lot of ecological disasters and needs to be tackled with utmost expediency (Azhar et al. 2019; ALOthman and Wabaidur 2019; Khan et al. 2020). Exploring the possibilities of bio-based materials and bio-composites, which are in line with the values of sustainability and cleaner production, is essential to finding a solution to this problem (Tarani et al. 2021; AL-Oqla 2022; Fares et al. 2022). These materials are a viable replacement for traditional plastics because they are made from renewable resources (Hayajneh et al. 2022; AL-Oqla et al. 2022). Additionally, their right blending with environmentally friendly materials can improve their environmental performance and help reduce plastic waste (Al-Jarrah and AL-Oqla 2022). We can reduce the ecological threats brought on by plastic pollution and move toward a more sustainable future by embracing bio-based products and encouraging their use in a variety of applications (Al-Oqla et al. 2016; Wabaidur et al. 2020; Azam et al. 2022).

Activism against single-use plastic, particularly plastic straws, started in 2015 after videos arose of a turtle with a plastic straw in its nose and because of media interest in the garbage patch in the Pacific Ocean. Every year, 1 billion plastic straws are consumed in Greece. This enormous number emphasizes single-use plastic straws' significant environmental impact. Based on a recent political agreement between the European Parliament and the Council of the EU, single-use plastic straws have been excluded from the European market. The above decision "opens" a new market for more sustainable and environmentally friendly options in the production of drinking straws (Bouasker et al. 2014; James et al. 2019; Maraveas 2020; Al-Jarrah and AL-Oqla 2022; Rababah et al. 2022). Due to increased awareness of environmental impact issues, industrial policies and decision

Editorial responsibility: S.Fahad.

✉ E. Tarani
etarani@physics.auth.gr

[1] Laboratory of Advanced Materials and Devices, Department of Physics, Aristotle University of Thessaloniki, 54124 Thessaloniki, Greece

makers must balance the availability of raw materials with the performance of final products (AL-Oqla et al. 2015a, 2016; AlFaris et al. 2020).

Seven hundred million tons of the annual garbage produced in the European Union are post-harvest agricultural wastes (AL-Oqla et al. 2015b; Babenko et al. 2018). Post-harvest agricultural leftovers have numerous advantages, including being easily renewed, accessible, recyclable, biodegradable, and ecologically compatible (Al-Oqla et al. 2014; Mati-Baouche et al. 2014; Maraveas 2020). They also have beneficial specific strength, weight, and excellent thermal and acoustic qualities (de Lima Mesquita et al. 2018; Hýsková et al. 2020). Regenerative agriculture contributes to the soil's ability to retain carbon, opposing the current global trends reflecting on the concentration of carbon dioxide in the atmosphere (Boonniteewanich et al. 2014). So, drinking straws made of lignocellulosic materials have a great deal of potential for future success (Lee et al. 2018; Hýsková et al. 2020; AL-Oqla and Hayajneh 2022).

A natural agricultural waste product such as wheat straw has the potential to effectively displace common plastic drinking straws. It is a completely natural product that will naturally degrade. As a result, wheat straws derived from agricultural output require no energy, and as a plant, it seizes CO_2 during the stem elongation phase, as well as no chemicals during manufacturing. Although there is strict European and National Legislation for materials that come into contact with food, there are no European standards for the physicochemical properties of wheat straws.

"Staramaki" SCE (2019) is a Greek company in Kilkis that manufactures drinking straws from the stalk of the wheat plant that are fully compatible with European and National Legislation. They are completely ecological, biodegradable, compostable, BPA-free, and do not contain additives, chemicals, gluten, or any allergens. According to the procedure, the wheat stems are cut by hand using specially shaped stainless-steel scissors. Trimmed stems are placed in preheated stainless-steel soaking tanks, and the soaked stems are then placed inside the boiler tank. Water rinsing is used between each process step and at the end of the cycle. Industrial washing units fully automate the final washing process. Stems are then positioned inside the drying chamber, where fans are used to circulate hot air around them. Each stem is individually inspected before final packaging.

In this work, wheat post-harvest crop residues were gathered from Kilkis region of Central Macedonia in Greece and used to make "Staramaki" drinking straws. Staramaki is a 100% natural product that replaces disposable plastic straws in the best way possible. For comparison reasons, straws made from different materials (reed, bamboo, paper, and bioplastic) were presented. X-ray diffraction (XRD) and scanning electron microscopy (SEM) were used to characterize the materials' structural properties and their morphological properties on the surfaces, respectively. To determine if these straws have adequate performance for use as drinking straws, the water absorption of the various straws was evaluated. Finally, the thermogravimetric analysis (TGA) technique was used to study the thermal stability and thermal degradation of the materials studied.

Materials and methods

Materials

Three varieties of wheat collected from different areas in Greece by Staramaki SCE were used in this study. Additionally, five commercial brands of straws (names of the brands were excluded) were presented for comparison reasons. Staramaki is made from the leftover stalk after wheat grains are harvested; hence, it is a 100% natural product. The selection criteria for sample collections in this research included several factors. Firstly, the geographical location of the wheat samples was considered, specifically focusing on the Kilkis region of Central Macedonia in Greece. The specific locations within this region were as follows: A1 from Kilkis, K1 from Metalliko, and G1 from Gorgopi. Secondly, the variety of wheat was taken into account, specifically assessing the morphological characteristics of the stem, such as the thickness and length of the 2nd internode. Additionally, the harvest dates of the wheat samples were considered. It was noted that only winter wheat is sown in Central Macedonia. The A1, K1, and G1 samples were harvested in July 2020. With the use of special stainless-steel scissors, the wheat stems are cut by hand. After cutting, the stems are sterilized through the use of thermal methods. It is produced by a social cooperative based in a rural region that, going beyond mere profitability, benefits the environment and the local agricultural economy and offers labor inclusion opportunities for vulnerable groups of people. Table 1 lists straws of different varieties of wheat and straws made of cane, bamboo, paper, and bioplastic.

Table 1 Type of straws and raw materials

Name of straws	Raw material used	Characteristics
K1	Wheat	Staramaki
G1	Wheat	Staramaki
A1	Wheat	Staramaki
WS	Wheat	Wheat straws
ECRT1	Reed	Reed straws
BS	Bamboo	Bamboo straws
PS	Paper	Bio paper straws
BPS	Bioplastic	Biodegradable

Characterization methods

X-ray diffraction (XRD)

The X-ray diffraction (XRD) patterns of the prepared materials were recorded by a 2-cycles Rigaku Ultima + X-ray diffractometer (Rigaku Corporation, Shibuya-Ku, Tokyo, Japan) with CuKα radiation (1.5418 Å), using a step size of 0.05° and a step time of 2 s in Bragg–Brentano geometry, operating at 40 kV and 30 mA. The Bragg diffraction formula was used to calculate the inter-planar spacings (d):

$$n\lambda = 2d\sin\theta \tag{1}$$

where n is an integer indicative of the reflection order, λ is the wavelength of CuKα radiation ($\lambda = 1.5418$ Å), and θ is the diffraction peak.

The deconvolution of the X-ray diffractograms was performed using a Gaussian–Lorentzian function (Hindeleh and Johnson 1971) to separate the amorphous and the crystalline content and calculate the crystallinity percentage. According to the profile fitting process, the weight crystalline fractions of the prepared materials were calculated as follows:

$$X_c = \frac{A_{cr}}{A_{cr} + A_{am}} \times 100\% \tag{2}$$

where A_{cr} denotes the area under the crystalline peaks, and A_{am} refers to the area under the amorphous peak. In this work, the deconvolution of the X-ray diffractograms and R^2 values were calculated using Origin software. By applying this approach to the obtained data, we were able to calculate the crystallinity percentages for the prepared materials.

Physical properties: absorption (%)

The samples were submerged in drinking water, coca-cola, and fresh orange juice for the absorption experiments. The straws were immersed for 30 min in each solution. This test was performed using the same initial temperature and liquid height. Before the tests, the weight of each specimen was precisely measured using digital equipment. The masses were measured before and after immersion for each straw. The mixture's solvent was then removed by drying the studied materials for 12 h at 35 °C in a laboratory oven. This was followed by a comparison of the immersion observed in the Staramaki straws with straws made from other materials. Six samples for each specimen type were tested. The absorption was calculated by using (Kenawy et al. 2018; Alothman et al. 2020):

$$\text{Absorption (\%)} = \frac{w_f - w_i}{w_f} \cdot 100\% \tag{3}$$

where w_i is the sample's weight prior to immersion in the liquid and w_f is the sample's weight following that.

Scanning electron microscopy (SEM)

Scanning electron microscopy (SEM) micrographs of the surfaces of the studied straws were studied using a SEM JEOL JSM-7610FPlus Schottky model (Pleasanton, CA, USA). The specimens were carbon coated to provide good conductivity of the electron beam, and the operating conditions were an accelerating voltage of 20 kV, a probe current of 45 nA, and a counting time of 60 s.

Thermogravimetric analysis (TG)

Thermogravimetric analysis (TG) of the studied straws was carried out using a Labsys evo TGA/DSC 1150 SETARAM instrument (Caluire, France) by heating the samples from 25 to 750 °C in a 50 ml/min flow of N_2 at a heating rate of 10 °C/min. Samples (9 ± 0.5 mg) were placed in alumina crucibles, while an empty alumina crucible was used as a reference. Continuous recordings of sample temperature, sample weight, its first derivative, and heat flow were taken.

Results and discussion

Structural characterization of straws

The goal of this study is to determine a material with high added value using low-cost raw materials. For this reason, it compares wheat varieties collected in Greece by Staramaki SCE with other commercial straws made of reed, bamboo, paper, and bioplastic. It is possible to assess the practicality and potential of wheat-based straws as a practical and environmentally beneficial option on the market by contrasting the wheat varieties harvested by Staramaki with other commercial straws. Figures 1 and 2 show the XRD measurements of the various straw types used. According to Fig. 1a, the main peaks of Staramaki (K1, G1, and A1), WS (wheat), and RS (reed) straws appear at angles of $2\theta = 15.0°$, 16.5°, and 22.8°. These reflections correspond to inter-planar spacings (d) of 5.9061 Å, 5.3724 Å, and 3.9002 Å, respectively, based on Bragg's law (Eq. (1)). The PDF card for these samples is #50–2241, which corresponds to the cellulose sample (2003). Cellulose is a high molecular weight linear polymer consisting of D-glucopyranose linked by β-1,4-glycosidic linkages. The repeating unit of cellulose is cellobiose. Hydroxyl groups in cellulose macromolecules are involved in several intra- and intermolecular hydrogen bonds, resulting in various ordered crystal arrangements (Park et al. 2010).

Crystallinity is a key parameter that characterizes the internal structure of materials and plays a crucial role in determining their properties and performance (Tarani et al. 2023). In the context of this study, the degree of crystallinity

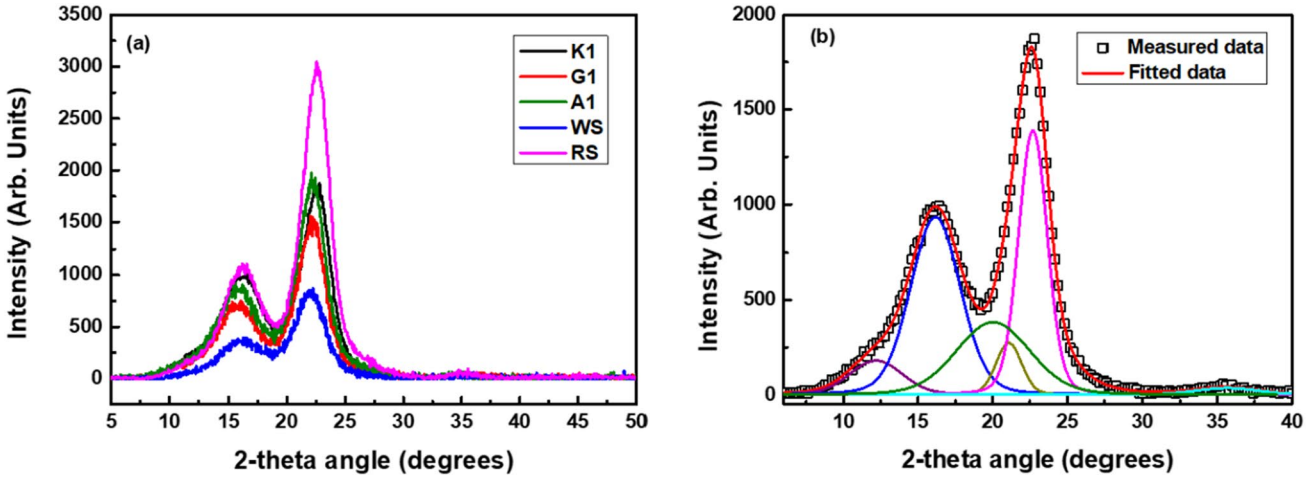

Fig. 1 **a** XRD diagrams of the cellulosic origin-type straws and **b** fitting method of selected experimental results

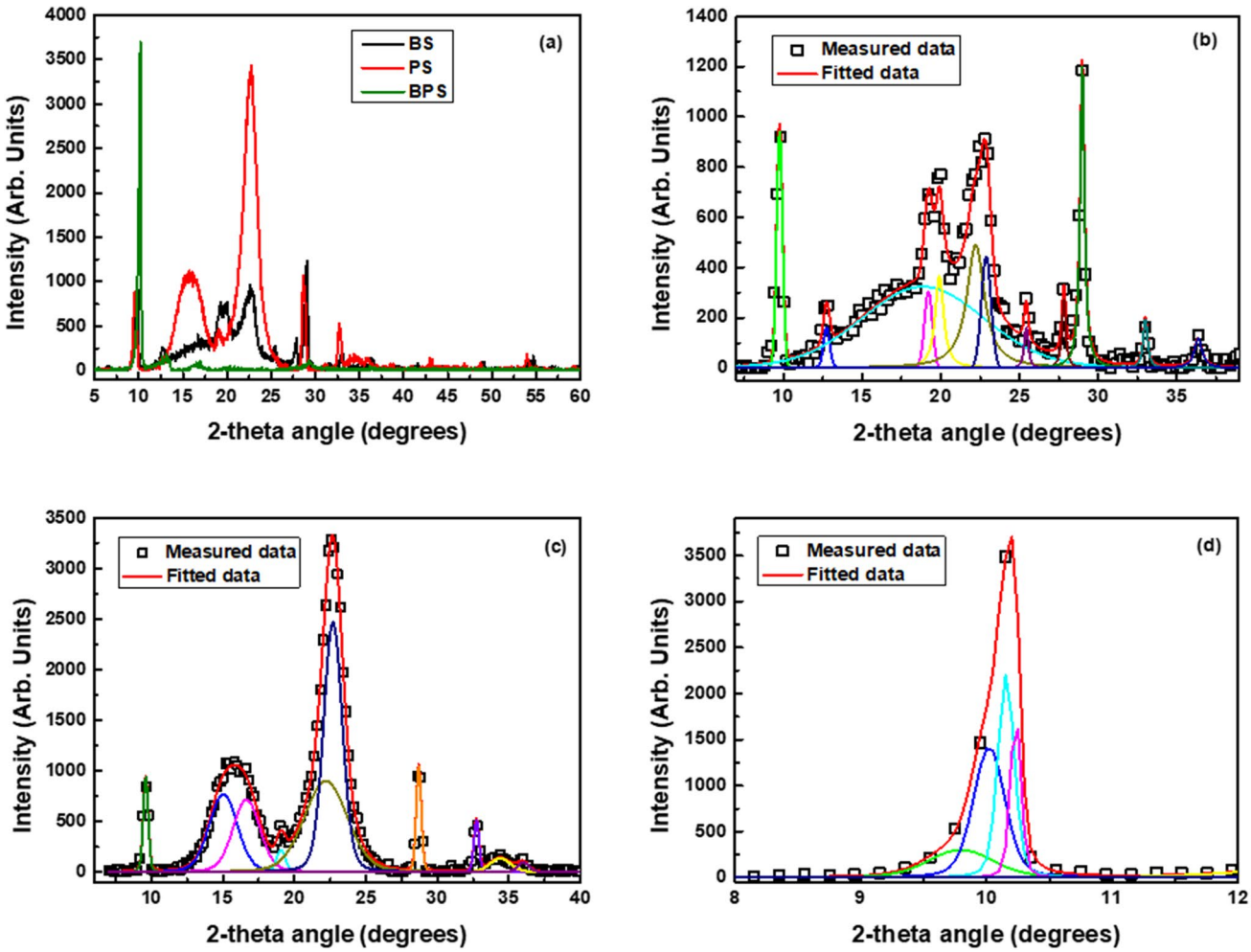

Fig. 2 **a** XRD diagrams of BS, PS, and BPS straws and experimental data fitting results for **b** BS, **c** PS, and **d** BPS straws

was investigated to assess the impact of different materials on the overall structural configuration of the straws; the higher the crystallinity, the greater the hardness and the lower the degree of water absorption (Chen et al. 2011; Jiang et al. 2020). To separate the amorphous and crystalline content and calculate the crystallinity percentage of the materials, a fitting of the experimental XRD results was performed using a combination of Gaussian–Lorentzian functions (Voigt function, Eq. (2)). This approach allows for the separation of the amorphous and crystalline components and enables the calculation of the crystallinity percentage. According to Table 2, the crystallinity values for wheat straws were found to be from 66.9 to 77.1% following the literature results (Park et al. 2010). The Staramaki K1 straw exhibits the highest crystallinity of all the straws analyzed, indicating a more structured and orderly arrangement of cellulose chains. According to Chen et al. (Chen et al. 2011), the presence of more stable cellulose chains results in a more crystalline structure, increasing thermal stability and strength.

Figure 2 shows the XRD patterns and the fitting results of BS (bamboo), PS (paper), and BPS (bioplastic) straws. In all cases, a wide band is observed, indicating a practically amorphous nature. The participation of the raw materials incorporated into the network of the cellulose polymer is obvious, leading to substantial changes in the structural configuration of the polymer matrix. In this case, the BPS straw presents the highest degree of crystallinity compared to the other ones.

Water absorption in straws

Figure 3 shows the change in mass for the Staramaki and straws made from other raw materials before and after immersion in water, coca-cola, and fresh orange juice at room temperature, Eq. (3). According to experimental results, the mass values of every straw increase after immersion, while the mass is approximately the same after drying. In detail, for the straws made from wheat, Staramaki straws (K1, G1, A1), and WS, an increase in mass was found after immersion in fresh orange juice of 41%, 55%, 71%, and 52%, respectively. The mass of K1, G1, A1, and WS straws increases by 67%, 108%, 128%, and 58%, respectively, after being submerged in coca-cola and by 40%, 62%, 77%, and 79% after being submerged in water. So, when immersed in solutions of fresh orange juice and coca-cola, the Greek-made K1 straw absorbs less liquid than the A1 and WS straws. Additionally, K1 and G1 straws return to approximately their initial mass after drying from the various solutions used. However, a change in mass of the A1 straw was found in 41 and 11% after drying from the fresh orange juice and coca-cola solutions, respectively. It seems that the 12 h at 35 °C is insufficient for this material to dry out after the immersion. Bouasker et al. (2014) reported that wheat straws can absorb a mass of water greater than their weight. According to Zheng et al. (2018), the increase in the porosity of the surface structure due to the partial degradation of hemicellulose and lignin allows the water molecules to penetrate the material. This results in high water absorption, which subsequently leads to increased swelling (Kain et al. 2014; Akinyemi et al. 2016).

From the straws made of reed, bamboo, paper, and bioplastic, it was found that BPS and BS straws, bioplastic, and bamboo straws maintain their mass. On the contrary, the PS straw made of paper has a relatively larger change in mass compared to other materials. It gained up to 41%, 56%, and 49% of its weight after immersion in water, coca-cola, and fresh orange juice, respectively. Gutierrez et al. (2019) reported that the paper straws absorbed liquid at approximately 30% of their weight after being exposed to liquid exposure for 30 min. It seems that the high water absorption causes significant swelling and shrinkage effects on the samples.

On the one hand, the increased acidity of the phosphoric acid present in cola can be used to explain the higher absorption seen in cola when compared to orange juice. The pH of phosphoric acid is known to be lower than the acids found in orange juice, such as citric acid. Due to its lower pH, phosphoric acid can break down the materials in the straw, making it corrosive and increasing its susceptibility to absorption. Additionally, coca-cola also has dissolved carbon dioxide gas because it is a carbonated beverage. Gas bubbles are added to the beverage during the carbonation process, and these bubbles may interact with the straws. These gas bubbles have the potential to enhance pressure, encourage the infiltration of water into the straw structure, and ultimately boost water absorption. On the other hand, orange juice's lower acidity and lower ion concentration may cause less interaction with the components of the straw, resulting in a lower level of absorption.

Table 2 Percentage of crystallinity of straws

A/A	Crystallinity (%)	R^2
K1	77.1	0.99916
G1	70.3	0.99744
A1	72.6	0.99865
WS	66.9	0.98919
RS	73.7	0.99871
BS	51.4	0.99227
PS	68.9	0.99740
BPS	88.5	0.99631

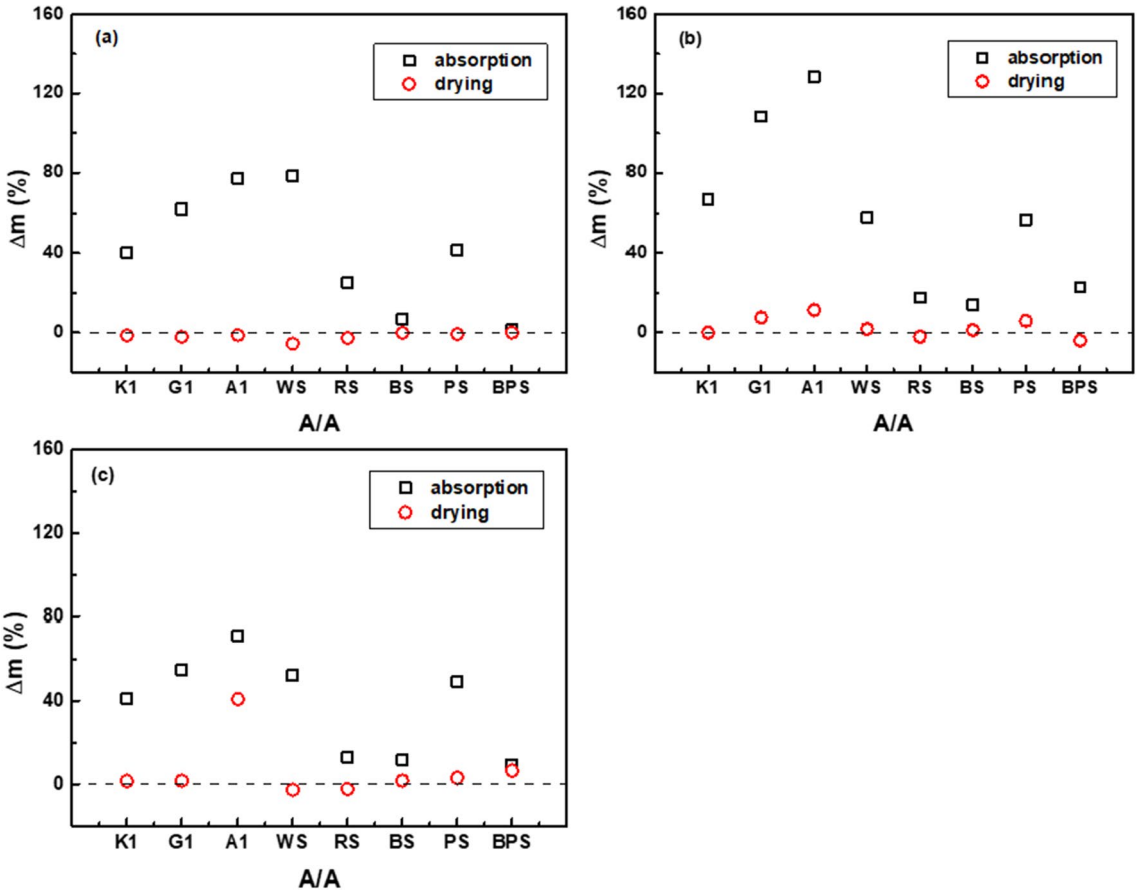

Fig. 3 Percentage mass change of straws before and after immersion and after drying in **a** water, **b** coca-cola, and **c** fresh orange juice. Optimal conditions: immersion at room temperature for 30 min, followed by drying at 35 °C for 12 h

Morphological characterization of straws

SEM was used to study the effect of water, coca-cola, and fresh orange juice solutions on the outer and inner surfaces of the various straws used. Figure S1 shows the SEM micrographs of the outer surface of the wheat straws before immersion. It has a distinctive shape where the pores in the top layer (epidermis) are sunk into the surface layer. A keratinous coating prevents slurry and admixture solutions from passing through the outside of wheat straw (Ghaffar et al. 2017; Farooqi and Ali 2018). As expected, it appears that Staramaki (A1, K1, G1), WS, and RS straws have a similar morphology. There are no voids in the specimens. This is consistent with the experimental results of XRD diagrams, in which the existence of cellulose was confirmed. Compared to WS, K1 and G1 straws have smaller slots and smoother outer surfaces, significantly lower than the four wheat straws. Figure S2 shows the SEM micrographs of the PS, BPS, and BS straws that appear to be more uneven and rough.

As mentioned above, the straws were immersed for 30 min in three solutions: (1) water, (2) coca-cola, and (3) fresh orange juice to study the effect of the components of each solution on the surface of the studied material. Figure 4 shows the SEM micrographs of the outer surface after immersion of different types A1, K1, and G1 of drinking straws at a 10 µm scale. The red marks observed in the micrographs are indicative of specific areas of interest, such as cracks, voids, and pores. The top layer (epidermis) of the wheat particle surface has lost some of its morphology in areas where pores are emerging. For water immersion, some cracks on the outer surface and material that has been peeled away from the main body of the straw can be seen. When the straws are immersed in water, the moisture can penetrate the outer surface and interact with the material. This may result in the material swelling and changing physically as a result. The swelling could cause layers to separate or crack, giving the illusion of material that has been peeled. Additionally, changes and cracks appear on the outer surface from the immersion of the straws in fresh juice and coca-cola; there are spots and areas of the surface that are a lighter shade of gray than the rest of the surface. As mentioned earlier, the acids in the juice and coca-cola can be highly corrosive and may play a role in the development of cracks or other surface

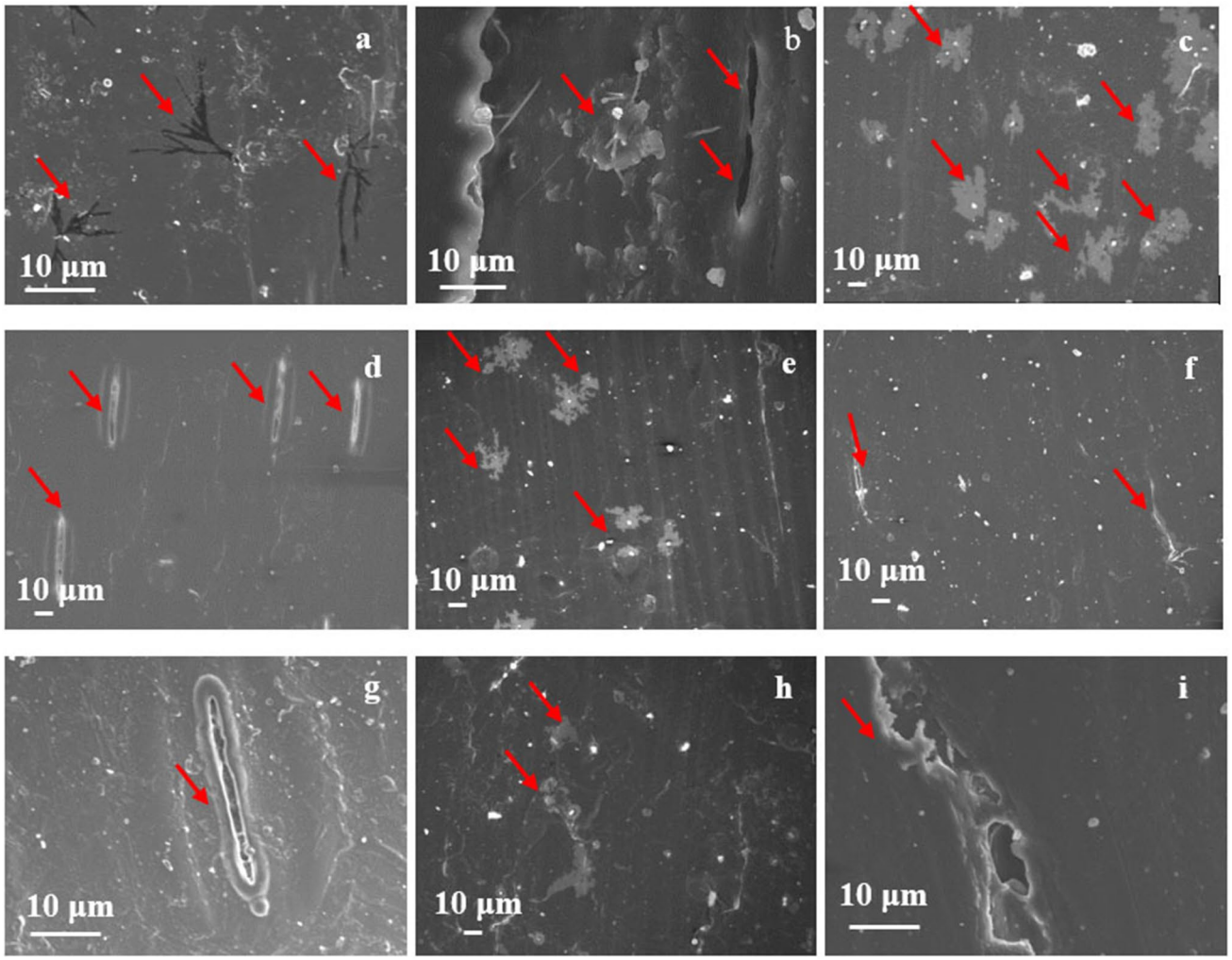

Fig. 4 SEM micrographs of outer surface of drinking straws after immersion in water, fresh juice, and coca-cola at 10 µm scale, **a–c** A1, **d–f** K1, and **g–i** G1 straws

alterations. Strong acids may react with the substance and cause surface erosion or degradation. It is possible that surface erosion or the elimination of material as a result of chemical reactions is the cause of the lighter shade of gray that is sometimes seen.

The same behavior was found for WS in Fig. S3 after its immersion in water, fresh orange juice, and coca-cola. So, wheat splits away from the main body, while air gaps, cracks, and WS porosity are visible during immersion in fresh juice and coca-cola, Fig. S3c, d–g of reed straws show that there are changes in the morphology of the outer surface, as well as some parts of the material that split away from its main structure. The SEM micrographs of the straw's surface reveal that there are different absorption properties due to the changes in roughness and structure of the straws.

Figure 5 shows the SEM micrographs of the paper, bamboo, and bioplastic straws. The micrographs indicate the separation and abscission of some tissues, the creation of cavities, and a rise in the surface roughness of the straws compared to those before immersion. Bamboo and bioplastic straws present damage to a lesser extent than the other ones, mainly peeling and deterioration caused by immersion in fresh juice and coca-cola. Additionally, the paper straws take on the color of the beverage, but they do not alter the liquid's aesthetic appearance. However, the interfacial bonding strength and the size of the gaps in paper straws lead to wet expansion and drying shrinkage. So, the destruction of outer surfaces results in higher water absorption, as previously revealed. Wheat straw soaks less than paper straw

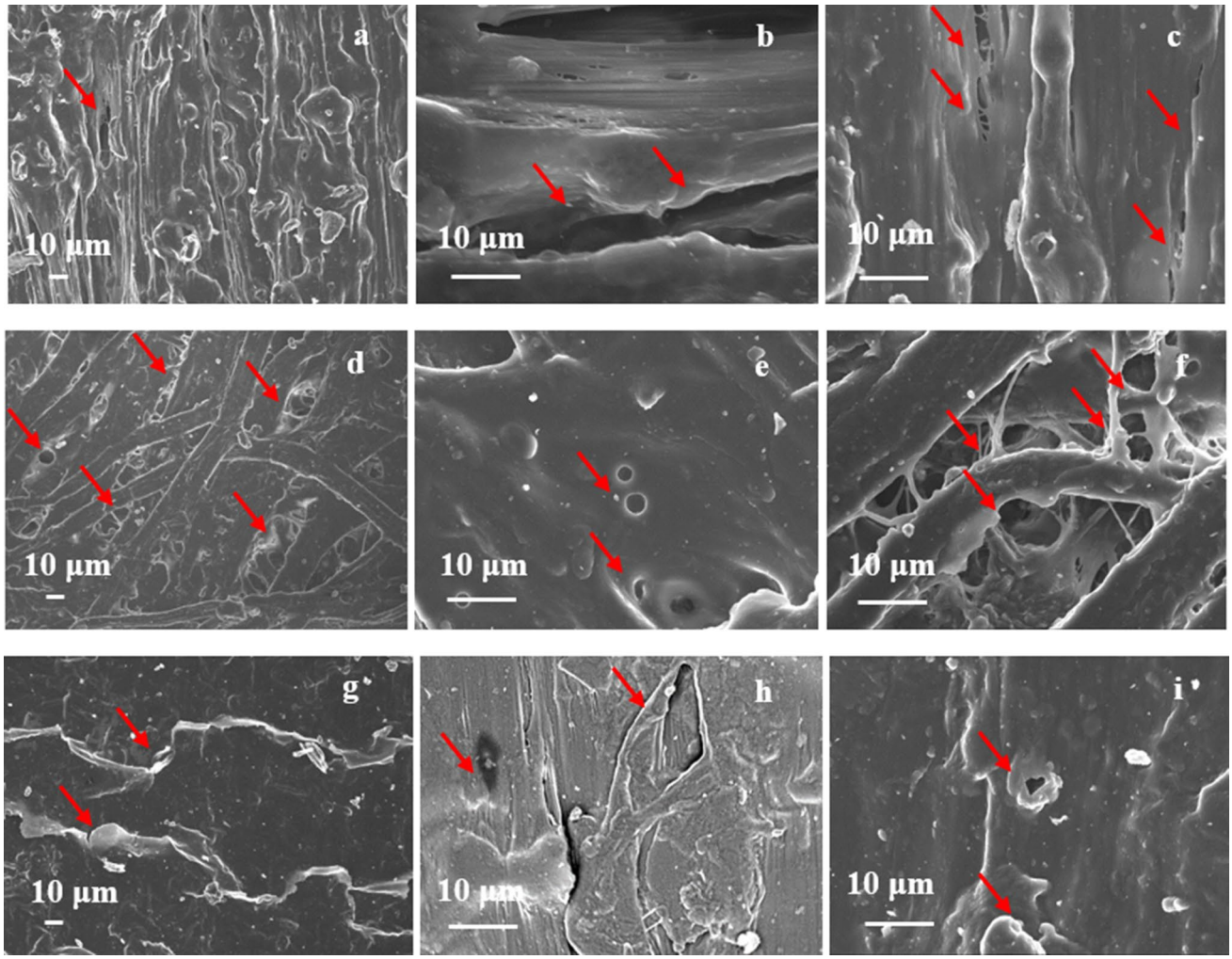

Fig. 5 SEM micrographs of outer surface of straws after immersion in water, fresh juice, and coca-cola at the 10 µm scale, **a–c** BS, **d–f** PS, and **g–i** BPS straws

because it is made from the stalks of the wheat plant rather than pulp.

Overall, the cracks, peeled material, and color changes on the straws' outer surface after exposure to water, fresh juice, and coca-cola are signs of the material's deterioration due to moisture, chemical interactions, and degradation processes. These modifications show how susceptible the straw material is to the particular elements and circumstances present in each immersion medium.

The inside surface of the straws before immersion was then examined using SEM micrographs. Figure S4 displays SEM micrographs at scales of 100 and 10 µm taken from the interior surface of wheat straws. The best wheat straw was found to be the Staramaki K1 because it has a smooth inner surface compared to the other ones. On the inner surface, there is a thin keratinous layer, and its roughness is superior to that of the outer surface. This aligns with the observation that the outer surface of the straws exhibits smaller slots and smoother textures, which are notably lower compared to the four wheat straws. However, the WS straw presents significantly protruding regions throughout the main inner surface of the material, with a length of about 10 µm, compared to K1, A1, and G1 straws. Figure S5 shows the inner surfaces of RS, BS, BPS, and PS straws before immersion. The bioplastic surface of BPS straw has the least roughness compared to that of the other surfaces, while bamboo has the highest roughness and shows irregular structures.

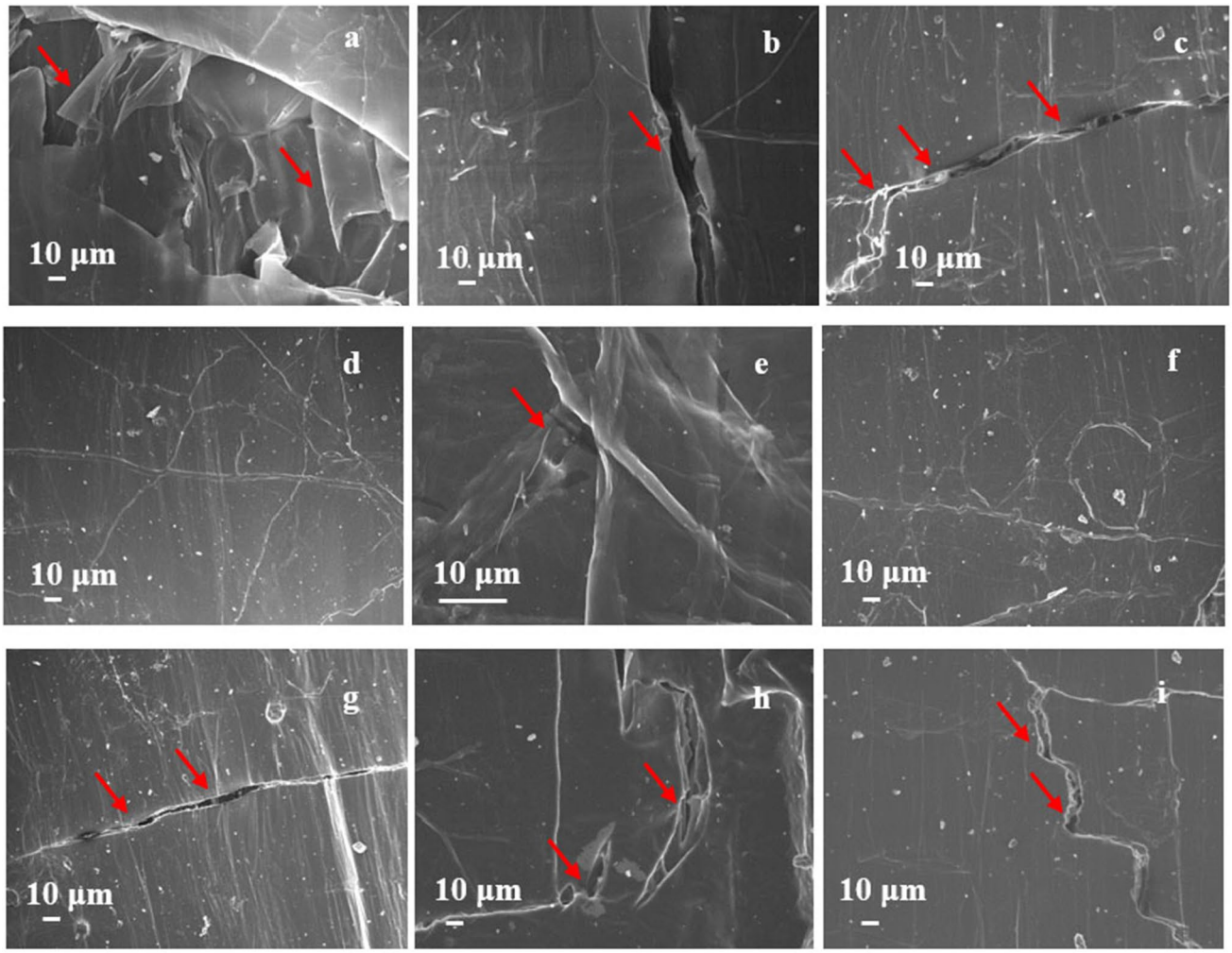

Fig. 6 SEM micrographs of inner surface of drinking straws after immersion in water, fresh juice, and coca-cola at a 10 µm scale, **a–c** A1, **d–f** K1, and **g–i** G1 straws

SEM micrographs were used to compare the inner surfaces of the various straws that were immersed in the different solutions. Figure 6 shows the SEM micrographs of the inner surface of the Staramaki (K1, G1, and A1) wheat straws. It appears that the various treatments have different effects on each straw's inner surface. According to Fig. 6e, coca-cola and water have barely affected the inner surface of the K1 straw, whereas the sample dipped in a fresh orange juice solution has abnormalities. However, a strong effect of all types of solutions on the inner surfaces of G1 and A1 was found, with the A1 straw showing the most changes and cracks after immersion. Figure S6 shows the SEM micrographs of WS and RS straws after immersion. As expected, this straw shows similar behavior to the previous ones as it comes from wheat. However, the cracks from the effects of all the solutions are more intense compared to the K1 and G1 straws. The differences in their structural characteristics can be used to explain how various straw samples react to the solutions. On the one hand, it was found that the Staramaki K1 straw presents the highest degree of crystallinity compared to the other straws, indicating a more organized and structured arrangement of cellulose chains within the material. This structural configuration may help increase the overall stability and resilience of the straw to changes brought on by the solutions. On the other hand, other straw samples present a less organized structure with more amorphous regions and lower levels of crystallinity. The less structured arrangement of molecular chains in the

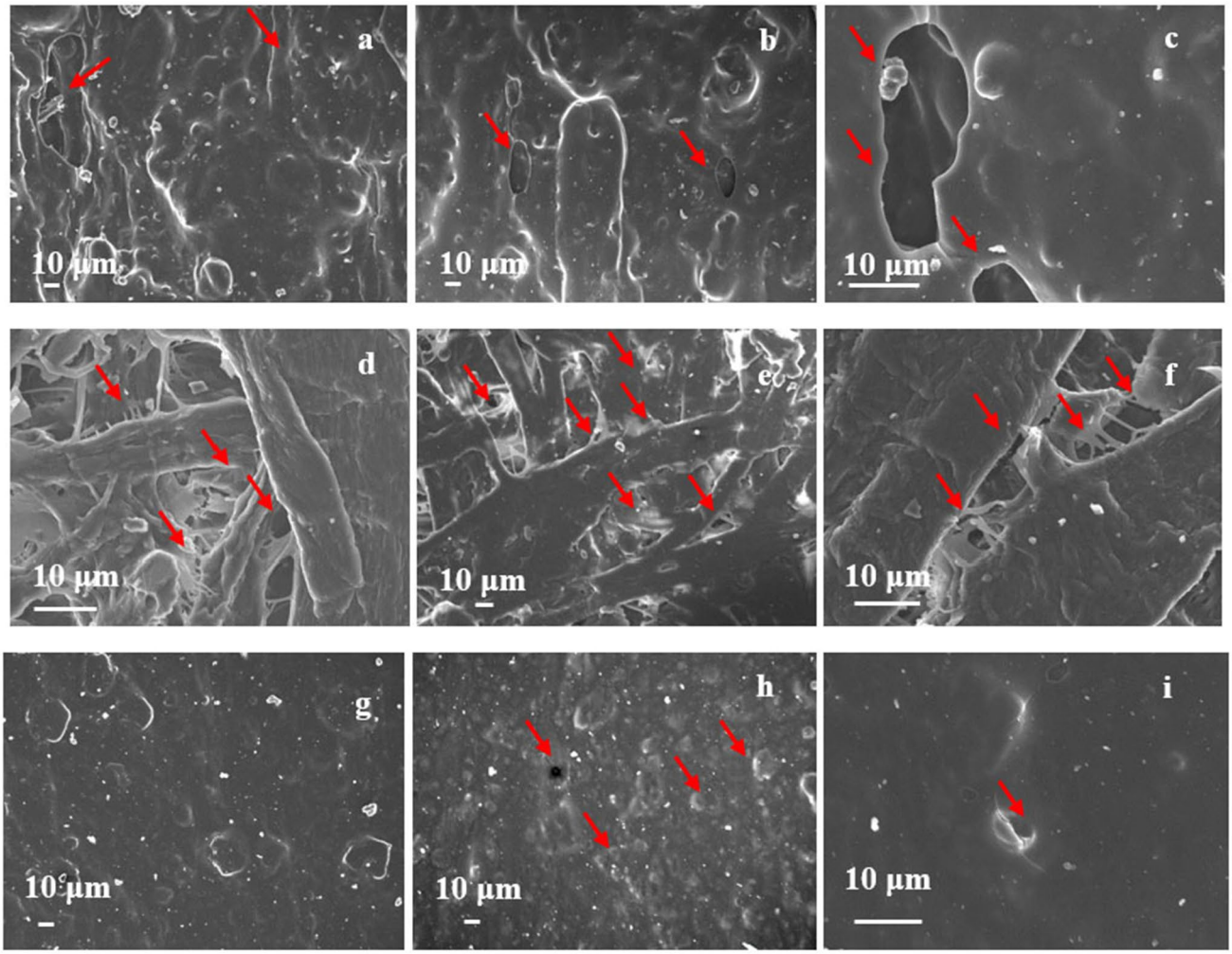

Fig. 7 SEM micrographs of inner surfaces of straws after immersion in water, fresh juice, and coca-cola, at a 10 µm scale, **a**–**c** BS, **d**–**f** PS, and **g**–**i** BPS straws

amorphous regions allows for greater interaction with the solutions, which could change the material's characteristics and appearance.

Figure 7 shows the SEM micrographs for BS, PS, and BPS straws. Some openings and breaks were found in BS straws due to the interaction with the solutions used, while the paper structure of the PS straws changed drastically, leading to the abscission of some sheets of paper. For the BPS straws, small cracks and changes can be seen in the form of small spots, with the fresh juice and coca-cola solutions being more intense than those of the water solution at the 10 µm scale. So, the presence of a highly crystalline structure can increase the straw's hardness and reduce its water absorption, making it more resistant to changes brought about by the solutions.

In comparison with the other raw materials, the Staramaki K1 wheat straw soaks less than paper as it is not pulp but comes from the stalks of the wheat plant. Additionally, the paper straws exhibit a phenomenon where the outer surface takes on the color of the liquid, they are immersed in. Furthermore, significant changes occur in the inner surface structure of the PS straws, resulting in the detachment of certain paper sheets. This highlights the environmental impact associated with the production of paper straws. The manufacturing process requires the destruction of mature forests to obtain the wood needed for pulp, which is then heavily processed before being transformed into the final paper product. Additionally, the BPS straw exhibits less absorption after being submerged in water, fresh orange juice, and coca-cola solutions. However, the CO_2 footprint

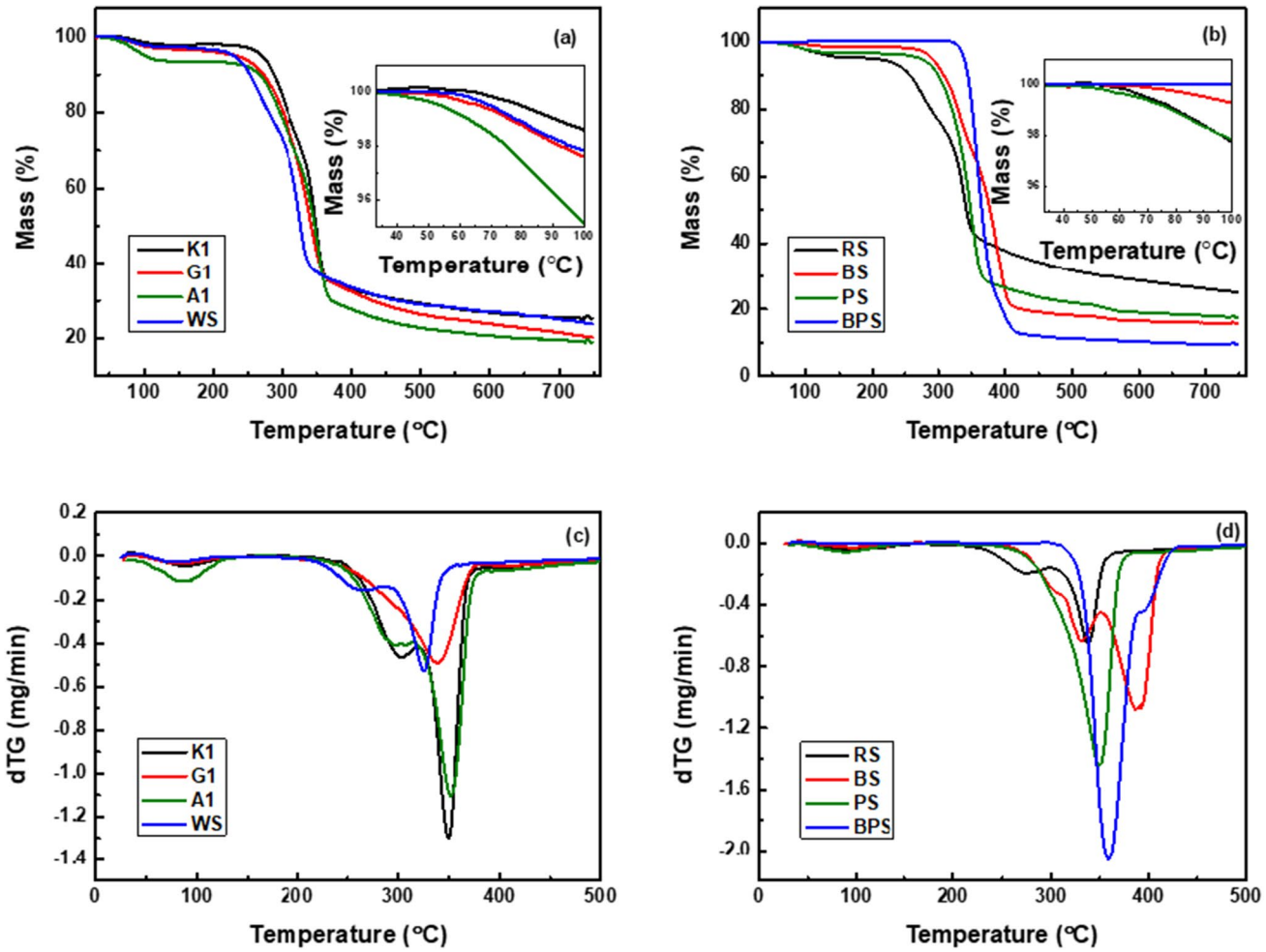

Fig. 8 TGA and DTG curves of the **a**, **c** wheat straws, and **b**, **d** other types of straws

of bioplastic straws is high due to waste during manufacturing (Boonniteewanich et al. 2014). In addition, in many cases, bioplastics do not break down any faster than regular plastic. So, Staramaki K1 straw demonstrates promising qualities for sustainable and eco-friendly alternatives in the straw industry.

Thermal properties of straws

Figure 8 shows the TGA plots of the change in mass as a function of temperature for the straws before immersion. These measurements were made to study the behavior of the materials with an increase in temperature if they are used in hot drinks. Figure 8a shows the change in mass of wheat straws and the corresponding area of interest under magnification (inset). The first stage (between 50 and 150 °C) is related to the initial weight loss caused by moisture evaporation and is strongly related to the initial moisture of samples. The severe weight loss caused by cellulose and hemicellulose degradation is referred to as the second stage (between 200 and 450 °C) (Bouasker et al. 2014; Chougan et al. 2020).

Samples K1, G1, A1, and WS show a similar trend in their thermal degradation, with differences in the quantitative part of the phenomenon. The K1 sample is more stable as the mass loss starts at higher temperatures compared to the other ones. Thus, an initial mass loss of 2% from 65 to 125 °C for K1 was found, while it remains constant until 242 °C. The enhanced thermal stability of straw and the high onset of degradation temperature are directly linked

(Ghaffar and Fan 2015). The cellulose crystallinity domains are thought to operate as barriers to heat transfer, possibly increasing thermal stability, which makes heat transfer more difficult in a more closed packing cellulose structure (Poletto et al. 2014). Kim et al. (Kim et al. 2010) showed that the thermal decomposition of cellulose shifted to higher temperatures with increasing crystallinity. The mass loss in WS begins at 52 °C and it has lost about 3% up to 97 ℃. Additionally, as shown in Fig. 8b, the BPS straw exhibits a constant value in mass change up to 330 ℃, where material decomposition begins, and complete degradation up to 410 ℃. Reed straws (RS) and paper straws (PS) show little thermal stability as their rate of mass change starts to decrease at lower temperatures than the other ones.

Figure 8c shows the derivative of the mass loss (DTG curves) of wheat straws, presenting the contribution of multiple decomposition events. This possibly indicates the presence of multiple degradation steps. The mass loss steps for all materials occur within the same temperature range. In detail, the first step of mass loss for all materials ranges from 45 to 140 ℃, the second step occurs between 220 and 320 ℃, and the final step is at 290–390 ℃. In Fig. 8d, it is observed that sample BPS shows a maximum at 360 ℃ in which there is a contribution of multiple decomposition events. Notable is the appearance of two maxima for the BS and RS straws, indicating that the decomposition starts at low temperatures and probably occurs in two steps. The PS straw shows decomposition at a lower temperature than the rest. Overall, all the straws exhibit good thermal stability, which qualifies them for hot beverages.

Conclusion

This study presents the efficacy of straws made of wheat as an alternative to plastic straws. Several experimental methods have been carried out, eventually leading the study of structural and morphological characterization, as well as physical properties. It was found that the K1 straw presents a more stable cellulose chain in the structure, leading to the highest degree of crystallinity and better thermal stability compared to the other ones. The water absorption properties of the straws were also investigated. The mass of each straw type increased after immersion in water, coca-cola, and fresh orange juice. The wheat straws exhibited significant mass increases after immersion, indicating high water absorption. The Staramaki K1 straw exhibits less absorption after being submerged in fresh orange juice and coca-cola solutions compared to the A1 and WS straws. The PS had the largest change in mass among the other materials, absorbing up to 41%, 56%, and 49% of its weight after immersion in water, coca-cola, and fresh orange juice, respectively. According to SEM micrographs, before immersion, the wheat straws had distinctive shapes with pores in the top layer and a keratinous coating. After immersion, the outer surfaces showed changes, cracks, and areas of lighter shades. The inner surfaces also exhibited various changes, with the Staramaki K1 straw being minimally affected, while the A1 and G1 straws showed more significant changes and cracks. The presence of a highly crystalline structure in Staramaki K1 can increase the straw's hardness and reduce its water absorption, making it more resistant to changes brought about by the solutions. Results from Staramaki straws, which are made from the stalk of the wheat plant and collected from various locations throughout Greece, show great potential for the development of a new class of environmentally friendly materials for drinking straws.

Supplementary Information The online version contains supplementary material available at https://doi.org/10.1007/s13762-023-05256-2.

Acknowledgements The authors would like to acknowledge Mrs Athina Taxintari, MSc., for her support. The publication of the article in OA mode was financially supported by HEAL-Link Greece.

Funding Open access funding provided by HEAL-Link Greece. This research received no external funding.

Declarations

Conflict of interest The authors declare no conflict of interest.

Ethical approval All authors confirm that the manuscript has been read and approved. All authors declare that this manuscript has not been published and not under consideration for publication elsewhere.

References

Akinyemi AB, Afolayan JO, OgunjiOluwatobi E (2016) Some properties of composite corn cob and sawdust particle boards. Constr Build Mater 127:436–441. https://doi.org/10.1016/j.conbuildmat.2016.10.040

AlFaris NA, Wabaidur SM, Alothman ZA et al (2020) Fast and efficient immunoaffinity column cleanup and liquid chromatography–tandem mass spectrometry method for the quantitative analysis of aflatoxins in baby food and feeds. J Sep Sci 43:2079–2087. https://doi.org/10.1002/jssc.201901307

Al-Jarrah R, AL-Oqla FM (2022) A novel integrated BPNN/SNN artificial neural network for predicting the mechanical performance of green fibers for better composite manufacturing. Compos Struct. https://doi.org/10.1016/j.compstruct.2022.115475

AL-Oqla FM (2022) Manufacturing and delamination factor optimization of cellulosic paper/epoxy composites towards proper design for sustainability. Int J Interact Des Manuf. https://doi.org/10.1007/s12008-022-00980-4

AL-Oqla FM, Hayajneh MT (2022) Stress failure interface of cellulosic composite beam for more reliable industrial design. Int J Interact Des Manuf 16:1727–1738. https://doi.org/10.1007/s12008-022-00884-3

AL-Oqla FM, Hayajneh MT, Al-Shrida MM (2022) Mechanical performance, thermal stability and morphological analysis of date palm fiber reinforced polypropylene composites toward functional bio-products. Cellulose 29:3293–3309. https://doi.org/10.1007/s10570-022-04498-6

Al-Oqla FM, Salit MS, Ishak MR, Aziz NA (2014) Combined multicriteria evaluation stage technique as an agro waste evaluation indicator for polymeric composites: date palm fibers as a case study. Bioresources 9:4608–4621. https://doi.org/10.15376/biores.9.3.4608-4621

Al-Oqla FM, Sapuan SM, Ishak MR, Nuraini AA (2016) A decision-making model for selecting the most appropriate natural fiber-Polypropylene-based composites for automotive applications. J Compos Mater 50:543–556. https://doi.org/10.1177/0021998315577233

AL-Oqla FM, Sapuan SM, Ishak MR, Nuraini AA (2015a) A model for evaluating and determining the most appropriate polymer matrix type for natural fiber composites. Int J Polym Anal Charact 20:191–205. https://doi.org/10.1080/1023666X.2015.990184

AL-Oqla FM, Sapuan SM, Ishak MR, Nuraini AA (2015b) Predicting the potential of agro waste fibers for sustainable automotive industry using a decision making model. Comput Electron Agric 113:116–127. https://doi.org/10.1016/j.compag.2015.01.011

Alothman ZA, Bahkali AH, Khiyami MA et al (2020) Low cost biosorbents from fungi for heavy metals removal from wastewater. Sep Sci Technol (philadelphia) 55:1766–1775. https://doi.org/10.1080/01496395.2019.1608242

ALOthman ZA, Wabaidur SM (2019) Application of carbon nanotubes in extraction and chromatographic analysis: a review. Arab J Chem 12:633–651

Azam M, Wabaidur SM, Khan MR et al (2022) Heavy metal ions removal from aqueous solutions by treated ajwa date pits: kinetic, isotherm, and thermodynamic approach. Polymers (Basel). https://doi.org/10.3390/polym14050914

Azhar A, Yamauchi Y, Allah AE et al (2019) Nanoporous iron oxide/carbon composites through in-situ deposition of prussian blue nanoparticles on graphene oxide nanosheets and subsequent thermal treatment for supercapacitor applications. Nanomaterials. https://doi.org/10.3390/nano9050776

Babenko M, Estokova A, Savytskyi M, Unčík S (2018) Study of thermal properties of lightweight insulation made of flax straw. Slo J Civ Eng 26:9–14. https://doi.org/10.2478/sjce-2018-0008

Boonniteewanich J, Pitivut S, Tongjoy S et al (2014) Evaluation of carbon footprint of bioplastic straw compared to petroleum based straw products. Energy procedia. Elsevier, pp 518–524

Bouasker M, Belayachi N, Hoxha D, Al-Mukhtar M (2014) Physical characterization of natural straw fibers as aggregates for construction materials applications. Materials 7:3034–3048. https://doi.org/10.3390/ma7043034

Chen X, Yu J, Zhang Z, Lu C (2011) Study on structure and thermal stability properties of cellulose fibers from rice straw. Carbohydr Polym 85:245–250. https://doi.org/10.1016/j.carbpol.2011.02.022

Chougan M, Ghaffar SH, Al-Kheetan MJ, Gecevicius M (2020) Wheat straw pre-treatments using eco-friendly strategies for enhancing the tensile properties of bio-based polylactic acid composites. Ind Crops Prod. https://doi.org/10.1016/j.indcrop.2020.112836

de Lima MA, Barrero NG, Fiorelli J et al (2018) Eco-particleboard manufactured from chemically treated fibrous vascular tissue of acai (Euterpe oleracea Mart.) fruit: a new alternative for the particleboard industry with its potential application in civil construction and furniture. Ind Crops Prod 112:644–651. https://doi.org/10.1016/j.indcrop.2017.12.074

Fares O, AL-Oqla F, Hayajneh M (2022) Revealing the intrinsic dielectric properties of mediterranean green fiber composites for sustainable functional products. J Ind Text 51:7732S-7754S. https://doi.org/10.1177/15280837221094648

Farooqi MU, Ali M (2018) Contribution of plant fibers in improving the behavior and capacity of reinforced concrete for structural applications. Constr Build Mater 182:94–107. https://doi.org/10.1016/j.conbuildmat.2018.06.041

Ghaffar SH, Fan M (2015) Differential behaviour of nodes and internodes of wheat straw with various pre-treatments. Biomass Bioenerg 83:373–382. https://doi.org/10.1016/j.biombioe.2015.10.020

Ghaffar SH, Fan M, McVicar B (2017) Interfacial properties with bonding and failure mechanisms of wheat straw node and internode. Compos Part A Appl Sci Manuf 99:102–112. https://doi.org/10.1016/j.compositesa.2017.04.005

Gutierrez JN, Royals AW, Jameel H, et al (2019) Paper vs. plastic straws

Hayajneh MT, Al-Shrida MM, Al-Oqla FM (2022) Mechanical, thermal, and tribological characterization of bio-polymeric composites: a comprehensive review. E-Polymers 22:641–663

Hindeleh AM, Johnson DJ (1971) The resolution of multipeak data in fibre science. J Phys D Appl Phys 4:259–263. https://doi.org/10.1088/0022-3727/4/2/311

Hýsková P, Hýsek Š, Schönfelder O et al (2020) Utilization of agricultural rests: straw-based composite panels made from enzymatic modified wheat and rapeseed straw. Ind Crops Prod. https://doi.org/10.1016/j.indcrop.2019.112067

James JJ, Silva DD, Varghese S et al (2019) Drinking straw from coconut leaf: a study of its epicuticular wax content and phenol extrusion properties. Asian J Plant Sci 18:139–147. https://doi.org/10.3923/ajps.2019.139.147

Jiang D, An P, Cui S et al (2020) Effect of modification methods of wheat straw fibers on water absorbency and mechanical properties of wheat straw fiber cement-based composites. Adv Mater Sci Eng. https://doi.org/10.1155/2020/5031025

Kain G, Güttler V, Barbu MC et al (2014) Density related properties of bark insulation boards bonded with tannin hexamine resin. Eur J Wood Wood Prod 72:417–424. https://doi.org/10.1007/s00107-014-0798-4

Kenawy ER, Ghfar AA, Wabaidur SM et al (2018) Cetyltrimethylammonium bromide intercalated and branched polyhydroxystyrene functionalized montmorillonite clay to sequester cationic dyes. J Environ Manage 219:285–293. https://doi.org/10.1016/j.jenvman.2018.04.121

Khan MA, Wabaidur SM, Siddiqui MR et al (2020) Silico-manganese fumes waste encapsulated cryogenic alginate beads for aqueous environment de-colorization. J Clean Prod. https://doi.org/10.1016/j.jclepro.2019.118867

Kim UJ, Eom SH, Wada M (2010) Thermal decomposition of native cellulose: influence on crystallite size. Polym Degrad Stab 95:778–781. https://doi.org/10.1016/j.polymdegradstab.2010.02.009

Lee SH, Ashaari Z, Ang AF et al (2018) Effects of two-step post heat-treatment in palm oil on the properties of oil palm trunk particleboard. Ind Crops Prod 116:249–258. https://doi.org/10.1016/j.indcrop.2018.02.050

Maraveas C (2020) Production of sustainable and biodegradable polymers from agricultural waste. Polymers (Basel) 12(5):1127

Mati-Baouche N, de Baynast H, Lebert A et al (2014) Mechanical, thermal and acoustical characterizations of an insulating bio-based composite made from sunflower stalks particles and chitosan. Ind Crops Prod 58:244–250. https://doi.org/10.1016/j.indcrop.2014.04.022

Park S, Baker JO, Himmel ME et al (2010) Open Access RESEARCH Cellulose crystallinity index: measurement techniques and their impact on interpreting cellulase performance. Biotechnol Biofuels 3:1–10

PC Powder Diffraction Files (2003) JCPDS-ICDD

Poletto M, OrnaghiJúnior HL, Zattera AJ (2014) Native cellulose: structure, characterization and thermal properties. Materials 7:6105–6119. https://doi.org/10.3390/ma7096105

Rababah MM, AL-Oqla FM, Wasif M (2022) Application of analytical hierarchy process for the determination of green polymeric-based composite manufacturing process. Int J Interact Des Manuf 16:943–954. https://doi.org/10.1007/s12008-022-00938-6

Staramaki (2019) https://www.staramaki.gr/

Tarani E, Arvanitidis I, Christofilos D et al (2023) Calculation of the degree of crystallinity of HDPE/GNPs nanocomposites by using various experimental techniques: a comparative study. J Mater Sci 58:1621–1639. https://doi.org/10.1007/s10853-022-08125-4

Tarani E, Patsiaoura D, Papadopoulou E et al (2021) A New textile economy: synthesis and characterization of phenolic type resin with protein from waste textiles suitable for wood-based panels. MDPI AG, p 15

Wabaidur SM, Khan MA, Siddiqui MR et al (2020) Oxygenated functionalities enriched MWCNTs decorated with silica coated spinel ferrite—a nanocomposite for potentially rapid and efficient decolorization of aquatic environment. J Mol Liq. https://doi.org/10.1016/j.molliq.2020.113916

Zheng Q, Zhou T, Wang Y et al (2018) Pretreatment of wheat straw leads to structural changes and improved enzymatic hydrolysis. Sci Rep. https://doi.org/10.1038/s41598-018-19517-5